

Chapter 3

The Riace bronzes: recent work on the clay cores

R. Jones¹, D. Brunelli², V. Cannavò², S.T. Levi², M. Vidale³

¹Archaeology, University of Glasgow, Glasgow, G12 8QQ, Scotland

²Dept. of Chemical and Geological Science, University of Modena and Reggio Emilia, Modena, Italy

³Dip. dei Beni Culturali: Archeologia, Storia dell'Arte, del Cinema e della Musica (DBC), University of Padua, Italy

Corresponding author: richard.jones@glasgow.ac.uk

Abstract

New samples of clay cores from the two Riace bronze statues have been analysed chemically, petrographically and by SEM to shed light on their origins. Sources in or around Corinth and Athens are excluded; the Argolid in the Peloponnese remains a possibility, and the Megarid should be considered further on geological grounds.

Keywords: *Riace bronzes, cores, chemical analysis, petrographic analysis, SEM, Peloponnese, Megarid*

Introduction

The famous mid-5th century BC bronzes found off the south east coast of Italy have deservedly received considerable art historical debate as well as the attention of programmes of conservation and restoration (Melucco and De Palma 2003) and analytical geosciences, reviewed by Dafas (2012). Known as Riace A and B (Fig. 1), these masterpieces represent heroes, probably warriors or athletes. Statue A differs from B in style, and possibly in some technical details. While the dates most commonly proposed considering the stylistic features are 460-450 and 440-430 BC respectively, a systematic campaign carried out at CEDAD (University of Salento, Italy) focused on the ¹⁴C AMS dating of 25 fragments of casting cores containing organic remains (13 for A, 12 for B). The conventional ¹⁴C dates for the two statues are safely included within the 5th century BC, quite coherent and essentially indistinguishable, but the flat shape of the ¹⁴C calibration between the 7th and 5th centuries BC prevents a finer dating (Calcagnile *et al.* 2010; Quarta *et al.* 2012). It is generally accepted that the upper limbs of B were replaced probably in the late Hellenistic or Roman period in a deliberate attempt to make it a twin of A, possibly for re-using the paired couple in a new architectural scenario.

Many researchers have used the composition characteristics of the casting clay cores found within the two statues to shed light on their compositional similarity, and for defining where the bronzes were manufactured (Quarta *et al.* 2012; Lombardi and Vidale 1998; Lombardi, Bianchetti and Vidale 2003; Formigli and Schneider 1993). On the basis of petrographic, chemical and palaeontological analyses, Lombardi and Vidale (1988) found substantial differences between the main casting cores of both statues and a special clay evidently

used for soldering the arms and the heads, and between the general core of statue B and the clay inside the allegedly modified right arm of B, circumstances fully verified by recent IBA compositional studies (Quarta *et al.* 2012). Lombardi and Vidale (1988, 1064) also concluded that southern Italy, large areas of Greece and the Aegean islands could be excluded as potential sources; Attica could not be ruled out and Argos presented the best affinity. Schneider (1989) was able to exclude Olympia as a source, and the same applied to southern Italy (Schneider and Formigli 2003). As to whether the two statues had the same origin, Lombardi and Vidale had proposed that “the basic materials of the two cores were gathered in two different micro-environments, but most likely belonged to the same geological basin”.

The aim of the new enquiry is to reconsider the origins of the statues' casting cores in the light of composition data for newly obtained core samples, in particular whether this data is consistent with possible origins in Corinth, Athens or Argos. As well as cores that were originally present when the statue was constructed, an important feature of the new sampling was the inclusion of not less than six cores from the right arm of Statue B which, as already mentioned, was a later addition. Another development is the analysis of two tiny black-varnish potsherds casually included in the casting cores, one in statue A, another in statue B.

Materials and methods

The samples of clay cores were removed from different inner parts of the two statues during the last conservative restoration in 1996. Twenty one of them (Table 1 and Fig. 1) were analysed in this work together with the two

sherds mentioned above. Fragments were crushed in an agate mortar yielding up to 500 mg powder which was then heated to 450°C for three hours, followed by chemical analysis by ICP-ES at the Department of Geosciences, Royal Holloway, London University. The concentrations of the thirty determined elements were examined using bi-variate plots and principal components analysis (with SPSS v.15).

Chemical results

The chemical compositions reveal some striking features. First, by comparison with Greek and south Italian pottery, the core castings in both statues have notably low aluminium and relatively low iron contents but very high calcium content. Second, the Ca-Al oxide plot (Fig. 2 left) clearly shows the difference between the two statues, confirming the general results of previous chemical studies. A2158 stands apart from the remainder owing to its very high iron content resulting from its proximity to an iron rod armature within the statue. It is also non calcareous, as are A2228 and A2233 which represent the separate (red) clay deliberately selected by the casters for its refractory property for the welding joints of the neck and armpits. The cores of B are strikingly calcareous and furthermore when viewed in multivariate space (Fig. 2 right) they are heterogeneous with B639 lying close to the main group of A cores. The cores from B have lower REE contents than those in A; apart from B639, they have high but wide ranging Sr contents which correlate with the corresponding Ca contents.

Furthermore four samples from the right arm of B - 648, 659, 662 and 663 - form a discrete group having low Ti, V, Y and REE contents; together with 654 they have in hand specimen a distinct crumbly texture and pale colour and furthermore these same five samples are rich in lead. They surely belong to the later replacement of the arm which was a leaded bronze (Giachetti *et al.* 1984, 85-106). However, 21, also from the right arm, emphatically belongs in terms of composition to the original cores of B (this different sample might come from a secondary intrusion). Both statues were originally cast with *unleaded* bronze (Mello 2003); the high copper content of some A cores (A2080, A2158, A2212, A2278) indicates that they were in contact with the bronze.

The distinctions in the origin sensitive elements, Co and Ni, between A and B are sufficiently small as to suggest a general similarity in origin. On the basis of the chemical data, we suggest one possibility: to the clay material used for A was added a (local) calcareous clayey soil to create the material for B. As regards the two sherds, the one in A has an Attic composition; that in B cannot yet be matched.

Petrographic results

The casting cores of the two statues have indeed quite homogeneous compositions; most of them have a fine-grained clay-carbonate matrix, although some differences

are attested in terms of grain size, porosity and inclusions. The bulk material of A is coarser than those of B, apart from the samples of the later restoration of the right arm from B which have a sand matrix (B663 and B648) or a coarse grained clay-carbonate matrix (B662, B659).

The grain size distribution is normally bimodal with different classes of clasts in the two statues. The inclusions in A range between 100-300 µm and 2-3 mm, with few exceptions up to 3-5 mm. The coarsest grain size distribution is attested in two anomalous samples, A2233 and A2228, collected from the left armpits. These cores are characterized by a reddish clay and frequent lithic fragments. The inclusions in B range between 50-100 µm and 300-600 µm; those at the high end of the range occur exclusively in the right arm samples.

The porosity is very low and mainly deriving by burning of organic inclusions and rare shrinkage cracks. The former, having the characteristic thin, curved, elongated shape of animal hair (up to 2 mm long) and rare vegetal fibres, are well suited to moulding effectively the clay in large concentric slabs. The main lithic inclusions are sedimentary rock fragments in association with low-grade metamorphic ones. The former are attested in both statues, in particular fine-grained carbonate rocks (naturally present in the clay mixture), chert and fine sedimentary quartzites. The metamorphic rocks are few and are composed of mica schists and quartzites. Igneous intrusive rocks are represented by clasts of deformed granitoids (quartz+mica) which should be indicative of granitic plutons in the sedimentary source area; we have not confirmed the presence of pyroclastic rocks which Lombardi and Vidale (1998, 1060) found among the samples they examined from statue A.

Calcite and quartz are the most abundant minerals; feldspars are present in lesser amount: plagioclase and microcline are recognizable only in B. Mica sheets (mainly composed of muscovite), pyroxenes and zircon are attested in some samples of both statues and they belong to the granitoids previously described. Rare epidotes are present in B. Iron oxides and opaque minerals are observed in all samples, and the latter were further investigated with SEM-EDS analysis. Other components of the casting cores are rare ARFs and grog fragments. Some metallic traces are also identified in the samples, depending on their position and distance from the casting flow.

Scanning Electron Microscopy

SEM examination of the casting cores of the two statues focused on rock minerals that could be provenance markers, in particular those associated with ophiolites, which outcrop in very limited areas of Greece. Secondary electron images (SEIs) of all samples show a significant amount of Mg-chromite (110 grains), zircon (220), the phosphate mineral monazite (Ce, La, Th)PO₄ (51) but fewer xenotime YPO₄ (10) (Figs. 3 and 4). Zircon is a common accessory mineral in many intrusive (especially granites and pegmatites) and sedimentary rocks.

Similarly, the accessory minerals, monazite and xenotime, point to the presence of evolved granitic bodies (pegmatites) in the source region, the former being frequently concentrated as a detrital mineral in stream and beach sand of intrusive and sedimentary rocks.

The zircon crystals in samples from both statues are generally small in size (<60 µm) but in differing amounts, except for the casting cores of the (replaced) right arm (B662, B663). The Mg-chromites are well attested in both statues but are prevalent in B. The crystals are often altered or cracked. The A samples are more enriched in monazite than in B, the highest concentration being attested in the left armpits, A2233 and A2228, which significantly also stand apart petrographically. The xenotime crystals are very small, making their identification difficult. There is a single example among the B casting cores (B635), and the others are identified in A2233, A2027, A2278, A2080, A2212 and A2158.

Discussion

On the basis of the data presented here, the hypothesis that A and B were constructed in the same general area of southern Greece remains, at present, the most likely. Here we review the evidence for the three possible sources.

Corinth area: combining our petrographic data set with those of Lombardi and Vidale (1998, 1064) and Whitbread (1995, 308-333), the case for an origin in the Corinth area is not strong. The statues contain more metamorphic rocks than are encountered at Corinth, and they lack clay pellets and mudstone which are common at Corinth. Chemically, the highly calcareous nature of most B cores finds some comparability with some pale-coloured clays due east of Acrocorinth (A in Fig. 5) examined by Newton *et al.* (1985) and Whitbread (2003, Fig. 1.1, 10). As regards the A cores, there are few if any chemical comparanda at Corinth (Jones 1986, Table 3.8). Instead the area to the east of Corinth may be more relevant in light of the presence in A of rock fragments indicative of ophiolites which outcrop in the Megarid (Fig. 5: ophiolitic rocks). Regrettably, there is no comparative chemical data for the Megarid.

Athens: petrographically, there are some resemblances with the geology of Attica, notably the metamorphic content, but the correspondence is not convincing. Although there are indeed calcareous clays in Athens, it is the consistently high Cr concentration, including significantly that in a core from the kouros statue of Piraeus analysed by Schneider (1989) (548 ppm Cr), which is the distinguishing feature of the pottery of Athens (and Attica). This feature is *not* shared by any of the Riace cores (94-235 ppm Cr).

Argos area: the identification by Lombardi and Vidale (2000, 1060) of serpentinite in some cores of statue A finds a possible match with the presence of flysch with associated outcrops of serpentine east of Argos (Shriner and Dorais 1999) (Fig. 6), but that association is not supported in the light of the results presented here: critically, optical and SEM investigation revealed ophiolitic rock fragments in the cores but not serpentine.

Modern bricks from Koutsopodi (8 km north of Argos) and from Argos itself have higher Al, Fe and Mn contents than in any of the cores (Jones 1986, 203).

In sum, although Corinth and Athens have been excluded, and southern Greece remains the most realistic possibility, the precise source (or sources) of A and B have not yet been confidently established. The Megarid needs to be considered further on geological grounds, although it is hard on archaeological grounds to accept such a source as the ophiolite in Fig. 5 borders the Alkyonides of the Gulf of Corinth – this is not a hospitable stretch of coast. The presence of granitoids instead – a feature that previous studies rather associated exclusively with the casting core of the substituted right arm of statue B – points to sources well away from the NE Peloponnese: parts of Macedonia, Samothrace, the Turkish Ionian coast, even the Cycladic islands of Mykonos, Delos and Naxos. The next stage of the project will include fieldwork in the Argos and Megarid areas, as well as characterisation of casting cores of bronze statues of known origin within Greece, such as at Argos, and beyond.

Acknowledgements

The project ‘Provenance study of melting clays from classical-age bronze casting’ was funded by CariModena Foundation and InResidence Design. Many thanks are also due to G. De Palma (ISCR, Rome) for her support to the current archaeometric studies on the Riace Bronzes. RJ thanks for Elizabeth Moignard for drawing attention to the study by Dafas (2012).

References

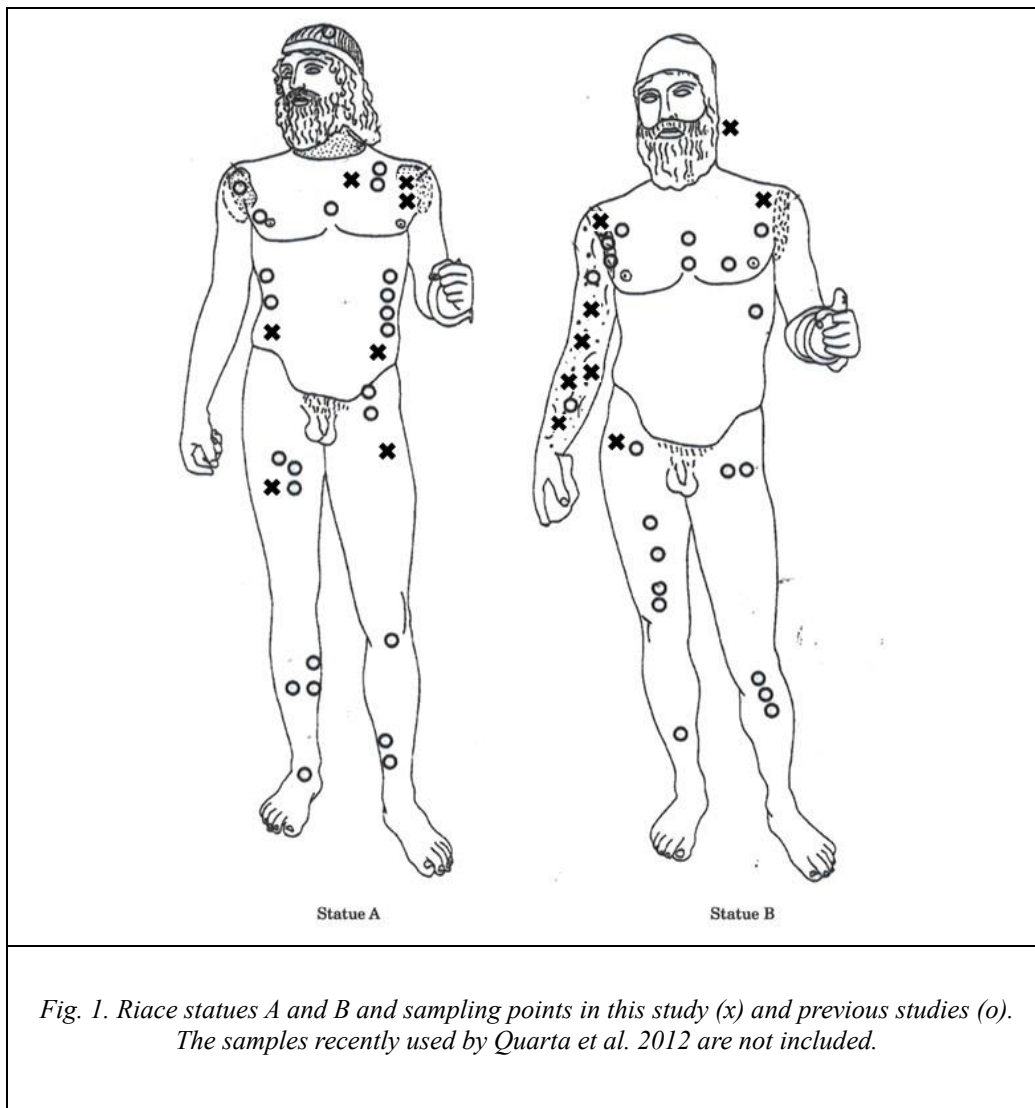
- Bornovas J. and Rondogianni-Tsiambou Th., 1983, *Geological map of Greece 1:500,000* 2nd ed., IGME, Athens.
- Calcagnile L, D’Elia M., Quarta G. and Vidale M., 2010, Radiocarbon dating of ancient bronze statues: preliminary results from the Riace statues, *Nuclear Instruments and Methods in Physics Research B*, 268, 20, 3356-3363.
- Dafas K., 2012, Greek large-scale bronze statuary revisited, Unpublished PhD thesis, King’s College London.
- Formigli E. and Schneider G., 1993, Antiche terre di fusione. Indagini archeometriche sulle terre di fusione di bronzi greci, romani e rinascimentali. In *Atti seminario studi ed esperimenti Murio 1991*, Siena, 69-102.
- Jones R.E., 1986, *Greek & Cypriot Pottery: a review of scientific studies*, Fitch Laboratory Occasional Paper 1, Athens.
- Lombardi G. and Vidale M., 1998, From the shell to its content: the casting cores of the two bronze statues from Riace (Calabria, Italy), *JAS* 25, 1055-66.
- Lombardi G., Bianchetti P.L. and Vidale M., 2003, Le Terre di fusione dei bronzi di Riace, in A.M. Vaccaro and G. de Palma (eds.) *I Bronzi di Riace:*

restauro come conoscenza I. Archeologia, Restauro, Conservazione, Roma, 131-80.

- Mello E., 2003, Studio metallografico, analitico, microanalitico e mediante tecniche spettroscopiche di analisi delle superfici di due campioni prelevati dalle statue di Riace, in A. Melucco Vaccaro and G. De Palma (eds.) *Restauro come Conoscenza I*. Istituto Centrale del Restauro, Artemide, Roma, 185-202.
- Melucco Vaccaro A. and De Palma A., 2003, *I bronzi di Riace: restauro come conoscenza*, Roma.
- Newton G.W.A., Robinson V.J., Oladipo M., Chandratillake M.R. and Whitbread I.K., 1988, Clay sources and Corinthian amphorae, in E.A. Slater and J.O. Tate (eds.), *Science and Archaeology, Glasgow 1987 conference*, Oxford: BAR 196, 59-81.
- Quarta G., Calcagnile L. and Vidale M., 2012, Integrating non-destructive ion beam analysis methods and accelerator mass spectrometry radiocarbon dating

for the study of ancient bronze statues, *Radiocarbon* 54, 801-812.

- Schneider G., 1989, Investigation of crucibles and moulds from bronze foundries in Olympia and Athens and determination of provenances of bronze statues, in Y Maniatis (ed.) *Archaeometry Proc. 25th Int. Symp.*, Amsterdam: Elsevier, 305-10.
- Shriner C. and Dorais M.J., 1999, A comparative electron microprobe study of Lerna III and IV ceramics and local clay-rich sediments, *Archaeometry* 41, 25-50.
- Whitbread I.K., 1995, *Greek Transport Amphorae: A petrological and archaeological study*, Fitch Laboratory Occasional Paper 4, Athens.
- Whitbread I.K., 2003, Clays of Corinth: the study of a basic resource for ceramic production, in C.K. Williams and N. Bookidis (eds.) *Corinth XX: Corinth, the centenary 1896-1996*, Princeton, 1-13.
- Zangger E., 1993, *The Geoarchaeology of the Argolid*, Berlin.



<i>Sample of Statue A</i>	<i>Description</i>	<i>Sample of Statue B</i>	<i>Description</i>
2027	Clay aggregations	2	Clast composed of slag
2080	Right leg (ht. 75-80 cm)	21	Right arm
2158	Filling of pit on right hip	236	Pottery sherd
2173	Chest	632	Left shoulder
2208	Pottery sherd	635	Right buttock
2212	Ht. 160 cm	641	Right shoulder
2228	Left armpit	648	Right arm
2233	Left armpit	654	Right arm
2238	Left hip	659	Right arm
2278	Left leg	662	Right arm
		663	Right arm
		671	Sporadic clay slab

Table 1. Casting cores samples and sherds from A and B.

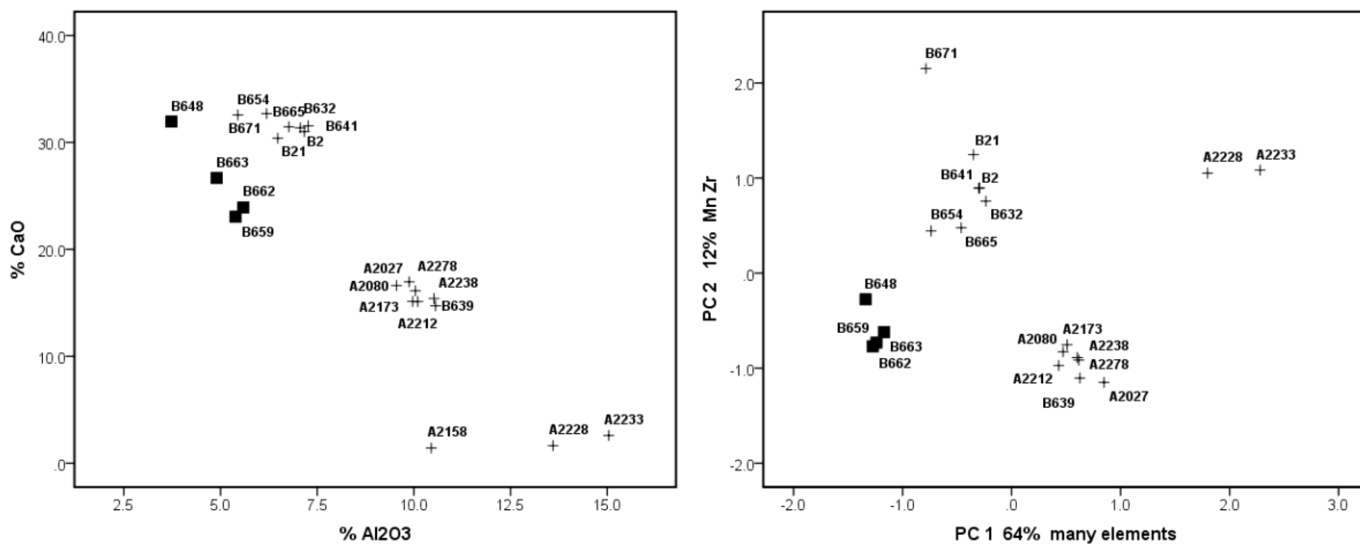


Fig. 2. Ca-Al oxide plot for all core casting (left). PC plot (right); all cores except A2158; samples from the replaced right arm of B are marked ■; all elements except Cu and Pb. PC1 is dominated by Al, Fe, K, Ti, Sc, V, La, Ce, Nd, Sm, Eu, Yb and Rb.

Sample number	Statue	Clasts %	Grain size	Clasts composition
2	B	1%	<50µm	Quartz, vegetal fibres, animal hair
21	B	3%	<2mm	Quartz, calcite, vegetal fibres, animal hair
632	B	1%	<50µm	Quartz, vegetal fibres, animal hair
635	B	3%	<600µm	Quartz, vegetal fibres, animal hair, mica
641	B	5%	<500µm	Quartz, plagioclase, calcite, arf, mica
648	B	20%	<2mm	Quartzite, quartzschist, quartz, calcite, feldspar, fossil
654	B	3%	<100µm	Quartz, plagioclase, calcite, mica, vegetal fibres, animal hair
659	B	20%	<1mm	Quartz, calcite, feldspar, quartz schist, srf
662	B	20%	<2mm	Quartz, calcite, feldspar, quartz schist, srf, chert
663	B	20%	<2mm	Quartz, calcite, feldspar, fossil, srf, crf, chert, mica schist
665	B	1%	<50µm	Quartz, vegetal fibres, animal hair
671	B	1%	<100µm	Mica, quartz, vegetal fibres, animal hair
2027	A	7%	<2.5mm	Crf, chert, mica, srf, vegetal fibres, animal hair
2080	A	5%	<3mm	Crf, chert, quartz, granitoids (quartz+mica), mica, srf, vegetal fibres, animal hair
2158	A	5%	<500µm	Quartz, mica, vegetal fibres, animal hair
2173	A	10%	<1mm	Crf, chert, mica, vegetal fibres, animal hair
2212	A	10%	<1mm	Quartz, calcite, quartzite, mica, vegetal fibres, animal hair
2228	A	15%	<800µm	Srf, chert, quartz, mica, vegetal fibres, animal hair
2233	A	15%	<3mm	Chert, quartz, granitoids (quartz+mica), mica
2238	A	5%	<700µm	Quartz, chert, vegetal fibres, animal hair
2278	A	7%	<500µm	Srf, chert, quartz, mica, vegetal fibres, animal hair

Table 2. Synthetic description of clasts in statues A and B: their percentage, grain size and composition. Arf argillaceous rock fragment; srf sedimentary rock fragment; crf carbonate rock fragment.

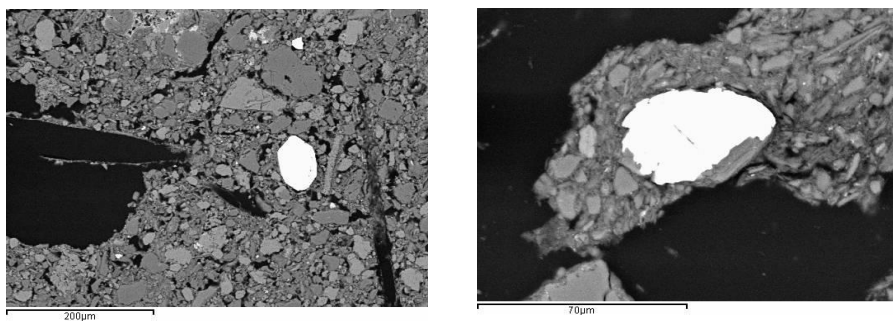


Fig. 3. Backscattered electron image of zircon (A2238, left) and monazite crystals (A2233, right).

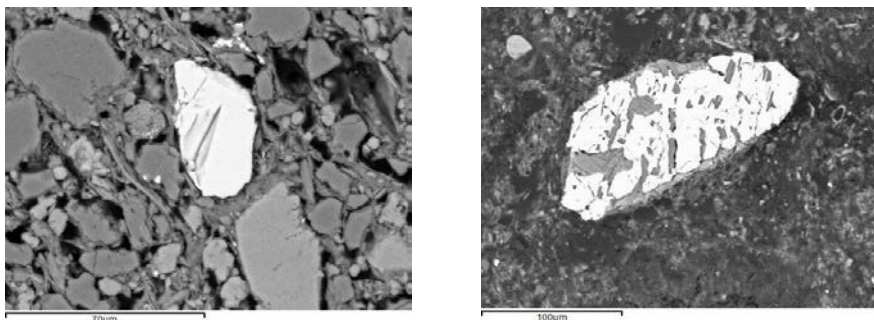


Fig. 4. Backscattered electron image of Mg-chromite from A (A2278, left) and B (B662, right).

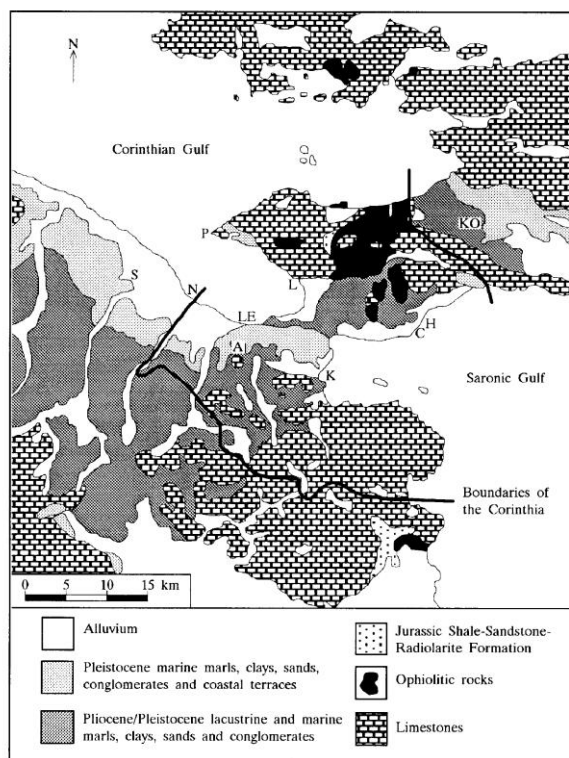


Fig. 5. Geological map of the Corinthia and Megarid (from Whitbread 1995, Fig. 5.2, after Bornovas and Rondogianni-Tsiambou 1983). A is Acrocorinth.

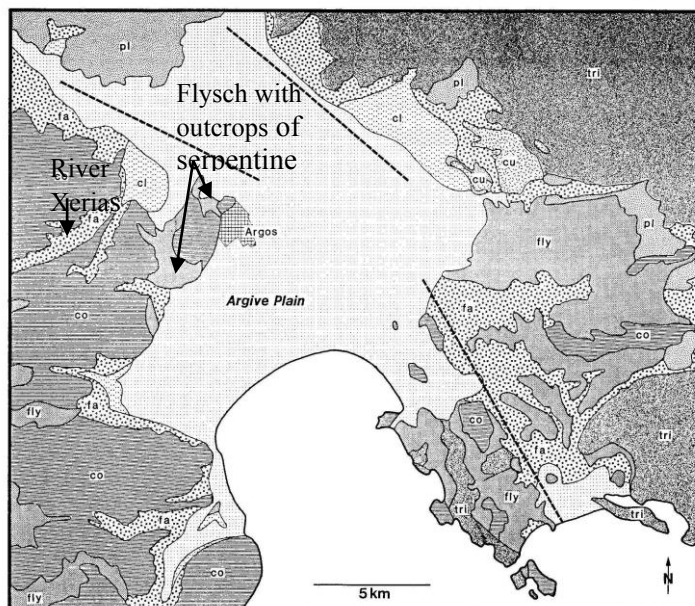


Fig. 6. The geology of the Argive Plain in the Peloponnese based on 1:50000 geological map of IGME, Athens (from Zangger 1993, fig. 6).